

Full Length Research Paper

Nonlinear Direct Torque Control of Interior Permanent Magnet Synchronous Motor Drive

Jackson J. Justo* and Francis Mwasilu

Department of Electrical Engineering, College of Engineering and Technology, University of Dar es Salaam, P.O. Box 35131, Dar es Salaam, Tanzania.

*Corresponding author: jackjusto2009@gmail.com

ABSTRACT

This paper presents a nonlinear direct torque control (NDTC) strategy of interior permanent magnet synchronous motors (IPMSMs) for electric vehicle (EV) propulsion. The proposed NDTC scheme applies a nonlinear model of IPMSM to dynamically determine the optimal switching states that optimize the EV drivers' decision to reduce the workload. Moreover, the proposed NDTC method has a simple control structure and can explicitly handle system constraints and nonlinearities. The performance evaluation is conducted via a prototype IPMSM test-bed with a TMS320F28335 DSP. Comparative experimental results provide the evidence of improvements of the proposed NDTC strategy over the conventional DTC strategy by indicating a fast torque response and an accurate speed tracking even under rapid speed change conditions.

Keywords: Direct torque control (DTC), interior permanent magnet synchronous motor (IPMSM), nonlinear direct torque control (NDTC).

INTRODUCTION

Interior permanent magnet synchronous motors (IPMSMs) have been considered as the potential candidates for electric vehicle (EV) applications due to their compact structure with small size and weight, high torque to current ratio, wide speed range, low noise, and robust operations (Justo *et al.*, 2017). They are also suitable for high-performance applications where high precision drives, such as in medical equipment or electronic devices manufacturing factories are required (Mohamed, 2007). Focusing on the EV-traction application, a fast and robust torque response of the IPMSM is required in a wide speed range to meet the instantaneous torque demand commanded

by the driver. Moreover, the IPMSM drive should have a quick torque/speed recovery capability after system disturbances and an insensitivity property to parameter variations. These are some of the requirements of the EV driver's torque/speed demand which must be achieved to match the vehicles cruising on internal combustion engines (ICEs) (Kolli *et al.*, 2013).

To enhance the steady-state and dynamic performances of the IPMSM drive, methods like the field-oriented control (FOC) with pulse-width modulation (PWM) are presented (Rahman *et al.*, 2004; Zhang and Zhu, 2011a). The quality of the FOC-PWM scheme depends on the performance of the outer and inner control

loops. One of notable drawbacks of this control scheme is the limited bandwidth which leads to an unsatisfactory control performance during transient-state with parameter uncertainties. Alternatively, a direct torque control (DTC) strategy has been presented for doing the same control tasks, and hence does away with the d - q axis current controllers (Xu and Rahman, 2012; Wallmark *et al.*, 2012; Xia *et al.*, 2014). Due to its simple structure, less parameter dependence, strong robustness against parameters variations, and quick dynamic response, the DTC scheme has been extended from induction machines to varieties of ac motor drives including the IPMSMs. The basic principle of the DTC method is to select the appropriate stator voltage vectors according to the error sign between the reference values and actual or estimated values of the torque and stator flux. However, high torque/flux ripples and variable switching frequencies which can be observed because of an included switching table are some of its disadvantages (Prior and Krstic, 2013; Zhang, 2013).

To overcome these drawbacks, improved DTC algorithms have been reported in the literature (Preindl and Bolognani, 2013a; Lee *et al.*, 2011; Foo and Rahman, 2010; Zhang, 2013; Zhao *et al.*, 2013). For instance, the basic DTC strategy can be integrated with a space vector modulation (SVM) (Preindl and Bolognani, 2013b). Different from the conventional one, the DTC-SVM generates a random voltage vector using any amplitude and length within its linear range. In this case, the torque and stator flux are regulated more accurately with a fixed switching frequency (Lee *et al.*, 2011; Foo and Rahman, 2010). It is worth to note that the DTC-SVM operating technique relies on how to select the firing voltage vector for a given sampling interval. Now, using deadbeat control (Zhang, 2013), indirect

torque control (Zhao *et al.*, 2013), and sliding mode control (Errouissi *et al.*, 2012) strategies, the DTC-SVM can be further improved to generate lower torque and stator flux ripples and fixed switching frequency. On the other hand, their constraints such as coordinate transformation, much knowledge of the motor parameters, and high computational burden, may negate their simplicity and robustness.

Recently, model predictive control (MPC) strategy, which can take into account the plant constraints and nonlinearities with multiple inputs/outputs and handle them in a proper way has been reported (Errouissi *et al.*, 2012; Preindl and Bolognani, 2013; Ma *et al.*, 2014). It generally has an optimal, naturally robust, and simple control structure. Thus, it can be combined with the basic DTC scheme to synthesize a high-performance controller for the Permanent Magnetic Synchronous Motor (PMSM) drives. Unlike the basic DTC or FOC with SVM, the DTC strategy is based on the optimal control approach (Cortes *et al.*, 2008). Having the cost function designed to minimize the torque and flux control errors (Li *et al.*, 2011; Chen *et al.*, 2014); optimized switching states can be generated. The technique is to minimize the electromagnetic torque error (i.e., T_{el}) and stator flux linkage error (i.e., ψ_s) by penalizing those errors using the weighting factors, τ and λ . However, it is not only a difficult but challenging and time-consuming problem to choose the exact values of the penalty factors at every sampling interval in order to obtain the optimized switching states. It is required to accurately anticipate the future operating behaviours of the plant along with the time for transient-state. Hence, tuning the weighting factors is still an open problem to find accurate and optimal solutions.

Therefore, this paper proposes a direct torque control (DTC) strategy based on a nonlinear direct control for the EV-traction using an IPMSM drive. Given the EV system dynamics and an objective cost function, the proposed NDTC strategy uses a nonlinear model to determine the optimal switching states similar to the EV drivers' decision and hence reducing the driving tasks. By employing the proposed NDTC scheme, the system complexity and nonlinearity can be easily handled to achieve a high-performance torque control for the EV traction with the IPMSM drive. The performance of the proposed scheme is validated by a prototype IPMSM test-bed with a Texas Instruments (TI) TMS320F28335 DSP.

METHODS AND MATERIALS

System Descriptions and Control Requirements

The major electrical components of the battery electric vehicle (BEV) traction as follows: i) an electric motor drive including a three-phase inverter and a drive train, ii) battery energy storage system (BESS), iii) charging system (i.e., charging plug, AC/DC converter, and DC/DC converter), and iv) EV central control system. Now due to the specific demand operation and varying on-road conditions, the electric motor drives are required to own some special characteristics, e.g., large torque output below its base speed, high efficiency in wide speed and torque ranges, etc. (Preindl and Bolognani, 2013b; Lee *et al.*, 2011; Foo and Rahman, 2010; Zhang, 2013).

In that perspective, the direct torque control (DTC) for EV traction applications is not a simple task in the sense that, the EV operation is essentially a nonlinear time-varying system (i.e., the EV

parameters and road conditions are always time-varying). Actually, there are some specific factors that make the EVs' performance lag behind the ICE vehicles (Kolli *et al.*, 2013; Rahman *et al.*, 2004; Zhang *et al.*, 2011) as follows: 1) Limited cruising range of only 100–200 km so far, and energy-saving strategy, 2) Charging and discharging rate, power train efficiency, and motion maneuverability, and 3) Overall system safety/protection and ride comfort. Therefore, to close these performance gaps, the DTC scheme for EV traction with an IPMSM drive should be designed with at least the following control requirements:

- a) Capability to maximize the efficiency of the motor drive over the whole speed range to extend cruising mileage for starting, rapid acceleration, cornering, and emergency braking (Kolli *et al.*, 2013; Chen *et al.*, 2014).
- b) Capability to safely ride-through during complicated operating conditions e.g., fault-tolerant control (Chen *et al.*, 2014).
- c) Ability to: i) regenerate power during braking (i.e., eco-driving or regenerative braking capability) (Li *et al.*, 2011) ii) recharge within a short time with a charge saving strategy so as to match the ICEs refuelling process (Chen *et al.*, 2014).

Control Requirements for Electric Vehicles

The direct torque control (DTC) for EV traction applications is not a simple task in the sense that, the EV operation is essentially a nonlinear time-varying system (i.e., the EV parameters and road conditions are always time-varying). These factors make the performance of the EVs trail the conventional internal combustion engines (ICEs) vehicles with respect to the following operating conditions (Kolli *et*

al., 2013; Rahman *et al.*, 2004; Zhang and Zhu, 2011b)

- Limited cruising range of only 100–200 km so far, and energy-saving mechanism.
- Charging and discharging rate, power-train efficiency, and motion maneuverability, and
- Overall system safety/protection and ride comfort.

Figure 1 shows that, in order to close these performance gaps, the DTC scheme for EV traction with an IPMSM drive should be designed with at least the following requirements:

- Proper controller to maximize the motor efficiency over the whole speed range to

extend cruising mileage while generating constant power above base speed for rapid acceleration (i.e., overtaking) and emergency braking with adaptive driving control.

- Easy control manoeuvrability to meet the required torque during starting, cornering, and climbing or descending.
- Capability to safely ride-through during complicated operating conditions e.g., fault-tolerant control (i.e., sensorless cruising mode).
- Ability to regenerate power during braking (i.e., eco-driving or regenerative braking capability).
- Capability to recharge within a short time and state-of-charge (SOC) saving strategy to match the ICEs refuelling process.

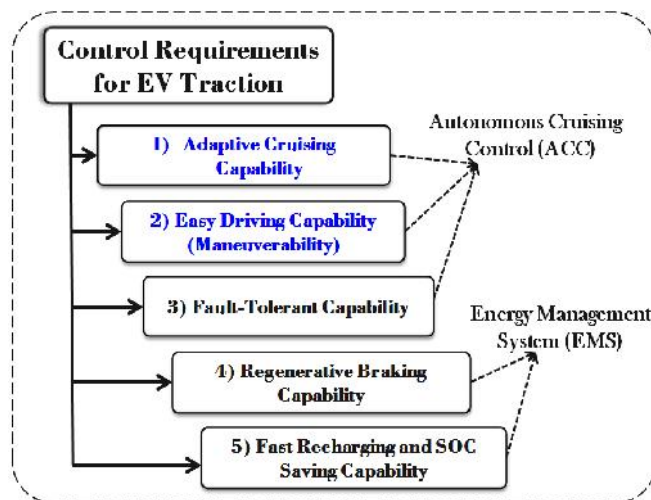


Figure 1: Requirements of the DTC strategy for EV traction with an IPMSM drive.

Control Requirement

When driving a car, the driver does not look immediately in front of his car, but he looks far ahead and changes the actuating variables such as the position of the steering wheel and brake before approaching on a red traffic light or a curved road portion. Besides, the driver initially calculates the behaviour of the car for a certain distance in front of him up to

a certain finite horizon taking into account the future values of the actuating variables. In such a pre-calculating process, decision optimization at every time instant is paramount i.e., during acceleration or braking according to the driving conditions. Likewise, in a real environment some different driving conditions may require a variable load torque demand which is realizable by the accelerator pedal action. The manoeuvrability of such a control action

requires a robust and adaptive nonlinear controller which instantly obeys the drivers' online/live requirements.

Therefore, to achieve such EV drive demands, a classical model predictive direct torque control (DTC), which more intuitively resembles a human physiological control, is first developed without considering the parameters variations. Thus, its control strategy is based on an explicit and identifiable model of the controlled system used to pre-calculate the behaviours of the controlled plant and choose an optimal value of the control variables. Next, a nonlinear DTC (i.e., NDTC) strategy is designed by considering the system uncertainties. The proposed NDTC treats the load torque variations as system disturbances and introduces an incremental weighing factor to improve its performance. Also, the NDTC is incorporated with stator flux and load torque estimators leading to a highly manoeuvrable control performance.

State space model of IPMSM with system uncertainties

A. Dynamic Model of IPMSM

Considering the Kirchhoff's voltage law (KVL) to the dq-axis equivalent circuits of a three-phase IPMSM, the following voltage equations in the synchronously rotating d-q reference frame are obtained:

$$V_{qs} = R_s i_{qs} + L_{qs} \dot{i}_{qs} + L_{ds} i_{ds} + \omega_m \lambda_m \dots\dots\dots (1)$$

$$V_{ds} = R_s i_{ds} + L_{ds} \dot{i}_{ds} - L_{qs} \omega_m i_{qs} \dots\dots\dots (2)$$

where V_{ds} and V_{qs} are the dq-axis voltages, i_{ds} and i_{qs} are the dq-axis currents, R_s is the stator resistance, L_{ds} and L_{qs} are the dq-axis inductances, ω_m is the electrical rotor speed, and λ_m is the magnetic flux.

Also, the electromagnetic torque can be obtained from the following electrical and mechanical equations:

$$T_e = \frac{3}{2} \frac{p}{2} [\lambda_m i_{qs} + (L_{ds} - L_{qs}) i_{ds} i_{qs}] \dots\dots\dots (3)$$

$$T_e = T_L + B \frac{2}{p} \dot{\theta} + J \frac{2}{p} \ddot{\theta} \dots\dots\dots (4)$$

where T_e and T_L are the electromagnetic and load torques, p is the number of poles, B is the viscous friction coefficient, and J is the rotor inertia.

Substituting equation (3) into equation (4) yields the following speed dynamic equation:

$$\ddot{\theta} = \frac{3}{2} \frac{p^2}{4} \frac{\lambda_m}{J} i_{qs} - \frac{B}{J} \dot{\theta} - \frac{p}{2J} T_L + \frac{3}{2} \frac{p^2}{4} \frac{L_{ds} - L_{qs}}{J} i_{qs} i_{ds} \dots\dots\dots (5)$$

Using equations (1) to (5), the dynamic model of the IPMSM can be expressed by equation (6).

$$\begin{aligned} \dot{\theta} &= A_1 i_{qs} - A_2 \dot{\theta} - A_3 T_L + A_{11} i_{ds} i_{qs} \\ \dot{i}_{qs} &= -A_4 i_{qs} - A_5 \dot{\theta} + A_6 V_{qs} - A_{10} \dot{\theta} i_{ds} \dots\dots\dots (6) \\ \dot{i}_{ds} &= -A_7 i_{ds} + A_8 V_{ds} + A_9 \dot{\theta} i_{qs} \end{aligned}$$

where

$$\begin{aligned} A_1 &= \frac{3}{2} \frac{1}{J} \frac{p^2}{4} \lambda_m, A_2 = \frac{B}{J}, A_3 = \frac{p}{2J}, A_4 = \frac{R_s}{L_{qs}}, \\ A_5 &= \frac{\omega_m}{L_{qs}}, A_6 = \frac{1}{L_{qs}}, A_7 = \frac{R_s}{L_{ds}}, A_8 = \frac{1}{L_{ds}}, \\ A_9 &= \frac{L_{qs}}{L_{ds}}, A_{10} = \frac{L_{ds}}{L_{qs}}, A_{11} = \frac{3}{2} \frac{1}{J} \frac{p^2}{4} (L_{ds} - L_{qs}). \end{aligned}$$

In considering the system uncertainties such as motor parameter variations, external disturbances, etc., the system model (6) can be rewritten as follows:

$$\begin{aligned} \dot{\theta} &= A_1 i_{qs} - A_2 \dot{\theta} + A_{11} i_{ds} i_{qs} - A_3 d_1 \\ \dot{i}_{qs} &= -A_4 i_{qs} - A_5 \dot{\theta} + A_6 V_{qs} - A_{10} \dot{\theta} i_{ds} - A_6 d_2 \\ \dot{i}_{ds} &= -A_7 i_{ds} + A_8 V_{ds} + A_9 \dot{\theta} i_{qs} - A_8 d_3 \end{aligned} \dots\dots\dots (7)$$

where d_1 , d_2 , and d_3 are uncertain components which represent the motor parameter variations and external

disturbances, respectively. That is, d_1-d_3 are given by

$$d_1 = -\frac{3p}{4} \Delta \lambda_m i_{qs} + \frac{2}{p} \Delta B \dot{\lambda} - \frac{3p}{4} (\Delta L_{ds} - \Delta L_{qs}) i_{ds} i_{qs} + T_L + \frac{2\Delta J}{p} \dot{\lambda},$$

$$d_2 = \Delta R_s i_{qs} + \Delta \lambda_m \dot{\lambda} + \Delta L_{ds} \dot{\lambda} i_{ds} + \Delta L_{qs} \dot{\lambda} i_{qs},$$

$$d_3 = \Delta R_s i_{ds} - \Delta L_{qs} \dot{\lambda} i_{qs} + \Delta L_{ds} \dot{\lambda} i_{ds}.$$

Remark 1: The uncertain components d_1 , d_2 , and d_3 are unknown. However, they are assumed to be bounded, i.e., there exist the constants χ_1 , χ_2 , and χ_3 which satisfy $|d_1| \leq \chi_1$, $|d_2| \leq \chi_2$, and $|d_3| \leq \chi_3$. These assumptions are reasonable because the variations of the motor parameters cannot be infinite.

B. State Space Model of IPMSM

Defining the state space variables as

$$x_1 = i_d, \quad x_2 = \dot{i}_1, \quad x_3 = i_{ds} - i_{dsd} \quad \dots \dots \quad (8)$$

where i_d and i_{dsd} are the desired values of i_d and i_{ds} , respectively. In this work it was assumed that i_d , i_{qs} , and i_{ds} are measurable and the external load torque (T_L) is unavailable.

In IPMSMs, the reluctance torque is available because of the existing saliency ($L_{qs} > L_{ds}$). If the desired d -axis current i_{dsd} is kept at zero, one cannot utilize the potential reluctance torque. Thus, in order to maximize the torque generation of the IPMSMs in the constant torque region and increase the efficiency of the IPMSM drives, the armature current should be controlled according to the maximum torque per ampere (MTPA) trajectory operation. In this technique, the d -axis current reference is given by (9) in accordance with Evvouisi *et al.* (2012).

$$i_{dsd} = -\frac{(L_{qs} - L_{ds})}{\lambda_m} i_{qs}^2 \quad (9)$$

By taking the derivative of (8) and using (7), the following results are obtained

$$\dot{x}_1 = x_2$$

$$\dot{x}_2 = -A_1 k_5 x_1 - A_2 x_2 + A_1 k_6 V_{qs} - A_1 k_5 \dot{\lambda} - A_1 A_{10} i_{ds} \dot{\lambda} - A_2 \dot{\lambda} + A_{11} (i_{ds} i_{qs} + i_{qs} i_{ds}) - A_1 k_4 i_{qs} - A_1 k_6 d_2 - A_3 \dot{d}_1 - \dot{\lambda} S_d$$

$$\dot{x}_3 = -A_7 x_3 + A_8 V_{ds} + A_9 \dot{\lambda} i_{qs} - A_8 d_3 - A_7 i_{dsd} - \dot{i}_{dsd}$$

..... (10)

It is therefore general to set the following equations

$$g_2 = -A_1 k_5 \dot{\lambda} - A_1 k_{10} i_{ds} \dot{\lambda} - A_2 \dot{\lambda} + A_{11} (i_{ds} i_{qs} + i_{qs} i_{ds}) - A_1 k_4 i_{qs} - A_1 k_6 d_2 - A_3 \dot{d}_1 - \dot{\lambda} S_d$$

$$g_3 = -A_8 d_3 + A_9 \dot{\lambda} i_{qs} - A_7 i_{dsd} - \dot{i}_{dsd}$$

(11)

Then the model (10) can be reduced to

$$\dot{x}_1 = x_2$$

$$\dot{x}_2 = A_1 k_5 x_1 - A_2 x_2 + A_1 k_6 V_{qs} + g_2 \quad \dots \dots \dots (12)$$

$$\dot{x}_3 = -A_7 x_3 + A_8 V_{ds} + g_3$$

From equation (12), the dynamic model of the IPMSMs can be expressed in the state space form:

$$\dot{x} = Ax + Bu + g \quad \dots \dots \dots (13)$$

where $x = [x_1 \quad x_2 \quad x_3]^T$

$$A = \begin{bmatrix} 0 & 1 & 0 \\ k_1 k_5 & -k_2 & 0 \\ 0 & 0 & -k_7 \end{bmatrix} = \begin{bmatrix} a_{11} & a_{12} & a_{13} \\ a_{21} & a_{22} & a_{23} \\ a_{31} & a_{32} & a_{33} \end{bmatrix},$$

$$B = \begin{bmatrix} 0 & 0 \\ 1 & 0 \\ 0 & 1 \end{bmatrix} = \begin{bmatrix} b_{11} & b_{12} \\ b_{21} & b_{22} \\ b_{31} & b_{32} \end{bmatrix}, u = \begin{bmatrix} u_1 \\ u_2 \end{bmatrix} = \begin{bmatrix} k_1 k_6 V_{qs} \\ k_8 V_{ds} \end{bmatrix}, g = \begin{bmatrix} 0 \\ g_2 \\ g_3 \end{bmatrix}$$

where u is the control input. Now, the goal of this study is to design a control law u for an uncertain linear system (13).

Design of proposed controller

In the dq-axis, the flux-linkage λ_d and λ_q can be expressed in the following vector form of equation (14).

$$\begin{bmatrix} \lambda_{ds}(k+1) \\ \lambda_{qs}(k+1) \end{bmatrix} = \begin{bmatrix} L_d & 0 \\ 0 & L_q \end{bmatrix} \times \begin{bmatrix} i_{ds}(k+1) \\ i_{qs}(k+1) \end{bmatrix} + \begin{bmatrix} \mathcal{E}_m(k+1) \\ 0 \end{bmatrix}$$

..... (14)

Considering the Park and Clarke transformations, i_d and i_q can be generated from the phase current vector as

$$\begin{bmatrix} i_d(k+1) \\ i_q(k+1) \end{bmatrix} = \begin{bmatrix} \cos(\theta_r(k+1)) & -\sin(\theta_r(k+1)) \\ \sin(\theta_r(k+1)) & \cos(\theta_r(k+1)) \end{bmatrix} \begin{bmatrix} -1/2 & -1/2 \\ \sqrt{3}/2 & -\sqrt{3}/2 \end{bmatrix} \begin{bmatrix} i_a^{k+1} \\ i_b^{k+1} \\ i_c^{k+1} \end{bmatrix} \rightarrow \dots \dots \dots (15)$$

Here the predicted rotor angle, $\theta_r(k+1)$ can be obtained using the trigonometric equation below:

$$\theta_r(k+1) = \arctan\left(\frac{\mathcal{E}_{qs}(k+1)}{\mathcal{E}_{ds}(k+1)}\right) \dots \dots \dots (16)$$

Now, the magnitude of the estimated stator flux, \mathcal{E}_s can be obtained by

$$\mathcal{E}_s^p(k+1) = \sqrt{(\mathcal{E}_{qs}(k+1))^2 + (\mathcal{E}_{ds}(k+1))^2} \dots \dots \dots (17)$$

On the other hand, the estimation of the electromagnetic torque can be developed in the dq -axis using the following expression:

$$T_{el}^p(k+1) = \frac{3}{2} p (\mathcal{E}_m^p(k+1) i_q^p(k+1) + [L_d - L_q] i_{ds}^{k+1} i_q^{k+1}) \dots \dots \dots (18)$$

Then the control input vector $c_m = [c_{qm} \ c_{dm}]^T$ can be selected based on the following transformation matrix:

$$c_m(k) = \frac{2}{3} V_{dc} \begin{bmatrix} \cos(\theta_r(k)) & -\sin(\theta_r(k)) \\ \cos\left(\theta_r(k) - \frac{2f}{3}\right) & -\sin\left(\theta_r(k) - \frac{2f}{3}\right) \\ \cos\left(\theta_r(k) + \frac{2f}{3}\right) & -\sin\left(\theta_r(k) + \frac{2f}{3}\right) \end{bmatrix} \begin{bmatrix} C_a(k) \\ C_b(k) \\ C_c(k) \end{bmatrix} \dots \dots \dots (19)$$

where $C_{abc}(k) = [C_a(k), C_b(k), C_c(k)]^T$ is the switching vector within the eight-elements set $\{[0,0,0]^T, [0,0,1]^T, [0,1,0]^T, [0,1,1]^T, [1,0,0]^T, [1,0,1]^T, [1,1,0]^T, \text{ and } [1,1,1]^T\}$.

Next, the design steps for the complete operation of the proposed NDTc strategy can be summarized by “Step 1 – Step 6” below.

Step 1. Measure the stator current $i_{abc}(k)$ and rotor position $\theta_r(k)$, then determine $i_d(k)$, $i_q(k)$, and $\theta_r(k)$.

Step 2. Obtain the prediction model $i_{ds}(k+1)$, $i_{qs}(k+1)$, then predict

$T_e(k+1)$ and $\theta_r(k+1)$ for all the possible $C_{abc}(k)$.

Step 3. Generate the references, T_e^* using the PI-speed control loop and θ_r^* .

Step 4. Evaluate the input control signals using (19) above.

Step 5. Determine the optimal switching state, $C_{abc-opt}(k)$ for driving the three-phase inverter.

Step 6. Set $k = k+1$. Go to Step 1.

RESULTS AND DISCUSSION

Figure 3 illustrates the overall block diagram of a prototype IPMSM drive used in simulation and experimental studies. In this figure, an IPMSM drive system consists of three main parts: a brake which generates the required driving torque, a three-phase IGBT inverter that provides the voltage pulses to the stator windings, and a TI TMS320F28335 DSP which executes the proposed NDTc algorithm. The rotor position information (θ_r) is extracted using an incremental encoder RIA-40-2500ZO with 2500 pulses per revolution. Also, the stator currents (i_{sb}, i_{sc}) are detected by using the Hall-effect current sensor LTS6-NP and are converted into digital values by the 12-bit A/D converters. For each sampling time T_s , the optimal switching signals $C_{abc-opt}(k)$ are determined.

The parameters used in simulation and experimental studies are listed as follows: Rated power, $P_{rated} = 390$ W; stator resistance, $R_s = 2.48$; q -axis stator inductance, $L_q = 113.91$ mH; d -axis stator inductance, $L_d = 74.98$ mH; equivalent rotor inertia, $J_m = 0.00042$ kg·m²; viscous friction coefficient, $B_m = 0.0001$ N·m·s/rad; dc-link voltage, $V_{dc} = 295$ VDC; number of poles, $p = 4$; magnetic flux linkage, $\psi_m = 0.193$ V·s/rad; sampling period, $T_s = 200$ μs.

Thus, to reflect the real driving conditions and the nonlinear behaviours of the EV-traction with an IPMSM drive, the following EV cruising scenarios were considered (Do *et al.*, 2014; Foo and Rahman, 2009; Miranda *et al.*, 2009).

- Scenario 1:** Steady-state operation at constant load torque.
- Scenario 2:** Rapid speed change at constant load torque.
- Scenario 3:** Load torque step change at constant speed.

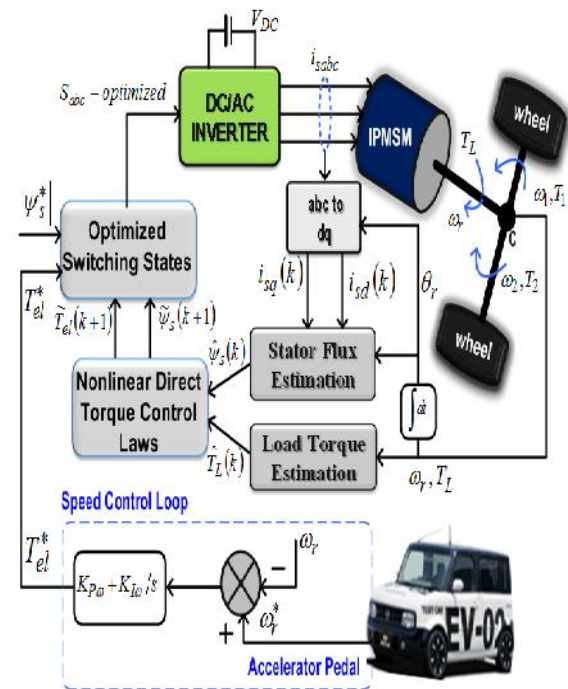


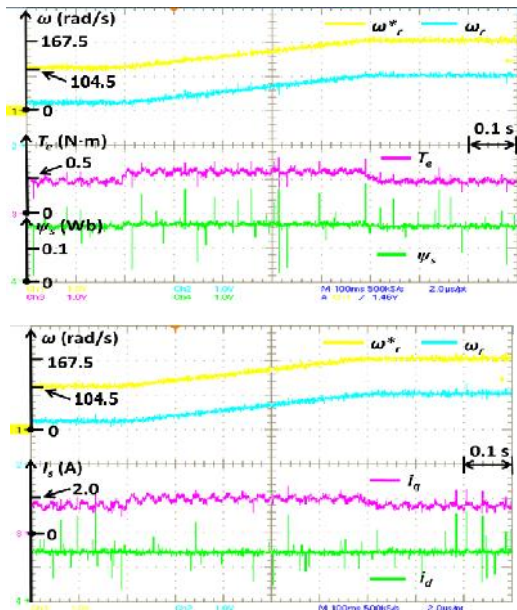
Figure 2: Overall block diagram of a prototype IPMSM drive used for experimental studies.

An experimental setup was designed to further validate the performance of the proposed NDTC scheme and the results are compared with those of the conventional DTC scheme. The studies are carried out under the same *Scenarios 1–3* as those considered in the simulation studies. First, the IPMSM speed trajectory was slowly changed from 104.5 rad/s to 167.5 rad/s at constant load torque of $T_L =$

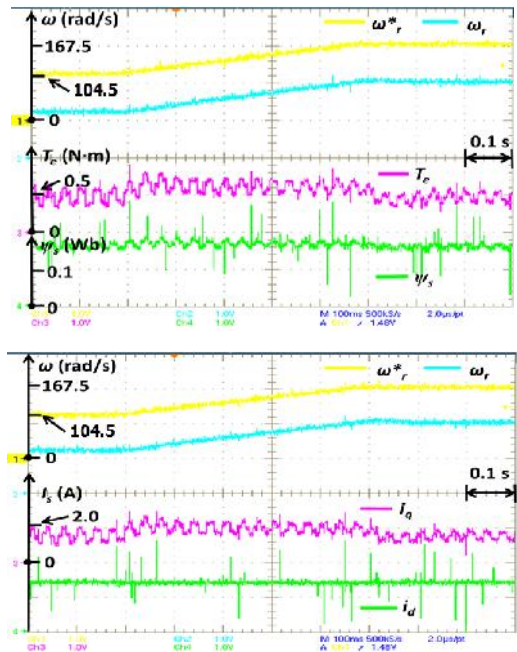
0.5 N·m, as shown in Figure 5. Under this transient-state, the dynamics of T_e and i_s respond according to the speed transient behaviour when the proposed NDTC scheme is applied. In Figure 3(a) and (b), i_q changes as the speed trajectory changes. Thus, the proposed NDTC strategy has a better overall performance with smaller oscillations than the conventional DTC scheme as indicated in Figure 3(a) and (b), respectively.

Next, the speed trajectory of 104.5 rad/s is rapidly changed to 313.5 rad/s while a constant load torque, $T_L = 1.2$ N·m is applied to validate the dynamic performance of the proposed controller (*Scenario 2*). From the transient responses indicated in Figure 4(a), the proposed NDTC strategy can still show excellent speed tracking performances with shorter settling time for speed, larger but shorter duration for i_d , i_q , and i_s overshoots than the conventional DTC scheme in Figure 4(b).

Finally, the third experimental study (*Scenario 3*) carries out the load torque perturbations from 0.5 N·m to 1.2 N·m when the speed trajectory is maintained at 251.3 rad/s. Thus, as shown in Figure 5(a), the proposed NDTC scheme indicates that the speed response is almost the same as its applied speed reference. Moreover, the responses of T_e , i_s , and i_q have shorter settling times and no oscillations during the transient time compared to the conventional DTC scheme. Alternatively, the performances of the conventional DTC scheme presented in Figure 5(b) for T_e , i_s , and i_q have longer settling times, and more oscillations compared to the proposed NDTC scheme.

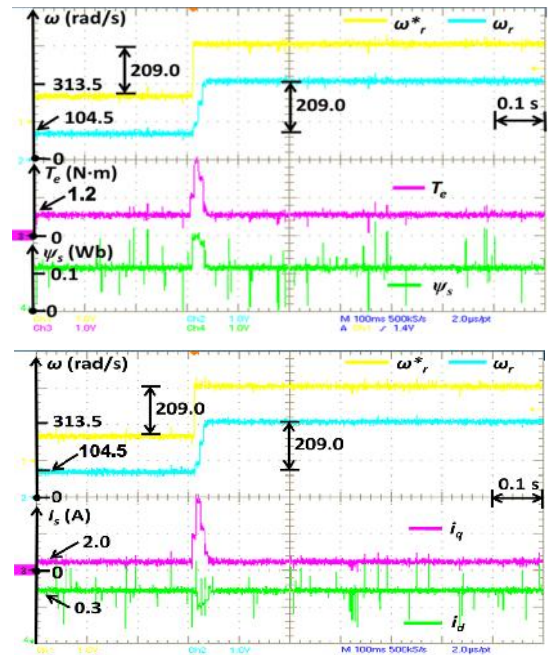


(a)

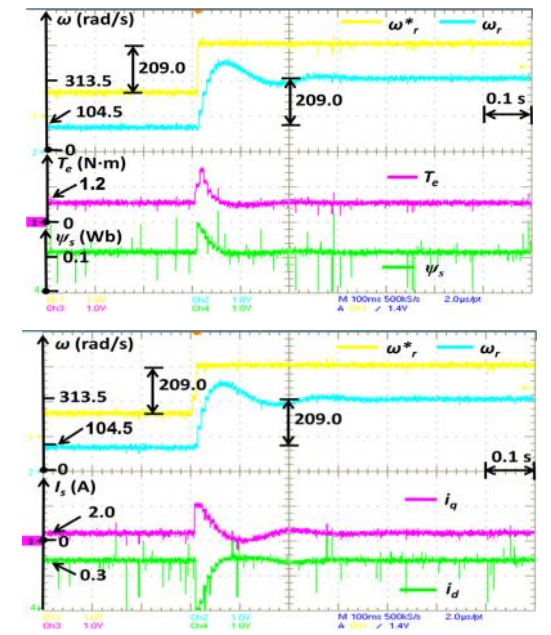


(b)

Figure 3: Experimental results under Scenario 1 (normal climbing condition) (a) Proposed NDTC strategy (b) Conventional DTC strategy.



(a)



(b)

Figure 4: Experimental results under Scenario 2 (i.e., overtaking situation) (a) Proposed NDTC strategy (b) Conventional DTC strategy.

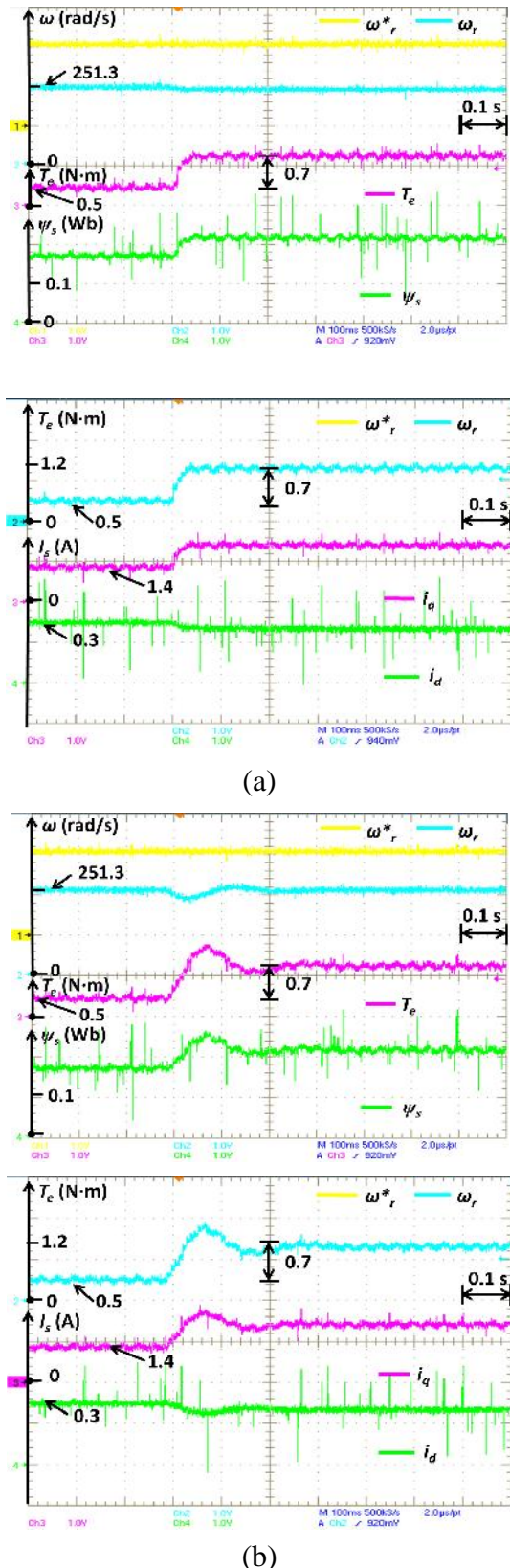


Figure 5: Experimental results under Scenario 3 (i.e., sudden climbing condition) (a) Proposed NDTC strategy (b) Conventional DTC strategy.

CONCLUSIONS

This paper proposed a nonlinear direct torque control (NDTC) strategy for the EV-traction with an IPMSM drive. By considering the nonlinear properties of the PMSM drive, the optimal switching states are generated which enhance the performance of the proposed NDTC scheme. Thus, the proposed scheme can precisely track the speed trajectory and guarantee a high performance even during the speed transients (i.e., normal and rapid speed change) or load torque step change. From the experimental studies, the proposed NDTC scheme demonstrated a fast speed tracking and precise torque response when compared with the conventional DTC scheme. Apart from generating optimal switching states which assists in improving the performance of the PMSM drive, the proposed NDTC scheme has a simple structure and preserves the advantages of the conventional DTC scheme.

REFERENCES

- Chen Y., Li X., Wiet C. and J. Wang (2014). Energy management and driving strategy for in-wheel motor electric ground vehicles with terrain profile preview. *IEEE Trans. Ind. Informat.*, 10(3): 1938–1947.
- Cortes P., Kazmierkowski M.P., Kennel R.M., Quevedo D.E. and Rodriguez J. (2008). Predictive control in power electronics and drives. *IEEE Trans. Ind. Electron.*, 55(12): 4312–4324. DOI: 10.1109/TIE.2008.2007480
- Do T.D., Kwak S., Choi H.H. and Jung J.W. (2014). Suboptimal control scheme design for interior permanent-magnet synchronous motors: An SDRE-based approach. *IEEE Trans. Power Electron.*, 29(6): 3020–3031.
- Errouissi R., Ouhrouche M., Chen C-W.H. and Trynadlowski A.M. (2012). Robust

- cascaded nonlinear predictive control of a permanent magnet synchronous motor with antiwindup compensator. *IEEE Trans. Ind. Electron.*, 59(8): 3078–3088.
- Foo G. and Rahman M.F. (2009). Direct torque and flux control of an IPM synchronous motor drive using backstepping approach. *IET Electr. Power Appl.*, 3(5): 413–421. DOI: [10.1049/iet-epa.2008.0182](https://doi.org/10.1049/iet-epa.2008.0182)
- Foo G.H.B. and Rahman M.F. (2010). Direct torque control of an IPM-synchronous motor drive at very low speed using a sliding-mode stator flux observer. *IEEE Trans. Power Electron.*, 25(4): 933–942. DOI: [10.1109/TPEL.2009.2036354](https://doi.org/10.1109/TPEL.2009.2036354)
- Justo J.J., Mwasilu F., Kim E.-K., Kim J., Choi H.H. and Jung J.-W. (2017). Fuzzy model predictive direct torque control of IPMSMs for electric vehicle applications. *IEEE Transactions on Mechatronics*, 22(4): 1542 - 1553. DOI: [10.1109/TMECH.2017.2665670](https://doi.org/10.1109/TMECH.2017.2665670)
- Kolli A., Bethoux O., De Bernardinis A., Laboure E. and Coquery G. (2013). Space Vector PWM control synthesis for an H-bridge drive in electric vehicles. *IEEE Trans. Veh. Technol.*, 62(6): 2441–2452. DOI: [10.1109/tvt.2013.2246202](https://doi.org/10.1109/tvt.2013.2246202)
- Lee J.S., Choi C.H., Seok J.K. and Lorenz R.D. (2011). Deadbeat-direct torque and flux control of interior permanent magnet synchronous machines with discrete time stator current and stator flux linkage observer. *IEEE Trans. Ind. Appl.*, 47(4): 1749–1958. DOI: [10.1109/TIA.2011.2154293](https://doi.org/10.1109/TIA.2011.2154293)
- Li S., Li K., Rajamani R. and Wang J. (2011). Model predictive multi-objective vehicular adaptive cruise control. *IEEE Trans. Control Syst. Technol.*, 19(3): 556–566. DOI: [10.1109/TCST.2010.2049203](https://doi.org/10.1109/TCST.2010.2049203)
- Ma Z., Saeidi S. and Kennel R. (2014). FPGA implementation of model predictive control with constant switching frequency for PMSM drives. *IEEE Trans. Ind. Informat.*, 10(4): 2055–2063. DOI: [10.1109/TII.2014.2344432](https://doi.org/10.1109/TII.2014.2344432)
- Mohamed Y.A.R.I. (2007). A newly designed instantaneous-torque control of direct-drive PMSM servo actuator with improved torque estimation and control characteristics. *IEEE Trans. Ind. Electron.*, 54(5): 2864–2873. DOI: [10.1109/TIE.2007.901356](https://doi.org/10.1109/TIE.2007.901356)
- Miranda H., Cortes P., Yuz J.I. and Rodriguez J. (2009). Predictive torque control of induction machines based on state-space models. *IEEE Trans. Ind. Electron.*, 56(6): 1916–1924. DOI: [10.1109/TIE.2009.2014904](https://doi.org/10.1109/TIE.2009.2014904)
- Preindl M. and Bolognani S. (2013a). Model predictive direct torque control with finite control set for PMSM drive systems, part I: Maximum torque per ampere operation. *IEEE Trans. Ind. Informat.*, 9(4): 1912–1921.
- Preindl M. and Bolognani S. (2013b). Model predictive direct speed control with finite set of PMSM drive systems. *IEEE Trans. Power Electron.*, 28(2): 1007–1015.
- Prior G. and Krstic M. (2013). Quantized-input control lyapunov approach for permanent magnet synchronous motor drives. *IEEE Trans. Control Syst. Technol.*, 21(5): 1784–1794. DOI: [10.1109/TCST.2012.2212246](https://doi.org/10.1109/TCST.2012.2212246)
- Rahman M.F., Haque Md. E., Lixin T. and Limin Z. (2004). Problems associated with the direct torque control of an interior permanent-magnet synchronous motor drive and their remedies. *IEEE Trans. Ind. Electron.*, 54(4): 799–809.
- Wallmark O., Lundberg S., and Bongiorno M. (2012). Input admittance expressions for field-oriented controlled salient PMSM drives. *IEEE Trans. Power Electron.*, 27(3): 1514–1520.
- Xia C., Zhao J., Yan Y. and Shi T. (2014). A novel direct torque control and flux

- control method of matrix converter-fed PMSM drives. *IEEE Trans. Power Electron.*, 29(10): 5417–5430. DOI:[10.1109/TPEL.2013.2293171](https://doi.org/10.1109/TPEL.2013.2293171)
- Xu Z. and Rahman M.F. (2012). Comparison of a sliding observer and a Kalman filter for direct-torque-controlled IPM synchronous motor drive. *IEEE Trans. Ind. Electron.*, 59(11): 4179–4188. DOI: [10.1109/TIE.2012.2188252](https://doi.org/10.1109/TIE.2012.2188252)
- Zhao Y., Qiao W. and Wu L. (2013). An adaptive quasi-sliding-mode rotor position observer-based sensorless control for interior permanent magnet synchronous machines. *IEEE Trans. Power Electron.*, 28(12): 5618–5629. DOI: [10.1109/TPEL.2013.2246871](https://doi.org/10.1109/TPEL.2013.2246871)
- Zhang X. (2013). Sensorless induction motor drive using indirect vector controller and sliding-mode observer for electric vehicles. *IEEE Trans. Veh. Technol.*, 62(7): 3010–3018. DOI: [10.1109/TVT.2013.2251921](https://doi.org/10.1109/TVT.2013.2251921)
- Zhang Y. and Zhu J. (2011a). Direct torque control of permanent magnet synchronous motor with reduced torque ripple and commutation frequency. *IEEE Trans. Power Electron.*, 26(1): 235–248. DOI:[10.1109/TPEL.2010.2059047](https://doi.org/10.1109/TPEL.2010.2059047)
- Zhang Y. and Zhu J. (2011b). A novel duty cycle control strategy to reduce both torque and flux ripples for DTC of permanent magnet synchronous motor drives with switching frequency reduction. *IEEE Trans. Power Electron.*, 26(10): 3055–3067. DOI:[10.1109/TPEL.2011.2129577](https://doi.org/10.1109/TPEL.2011.2129577)